

# Macaque Monoclonal Antibodies Targeting Novel Conserved Epitopes within Filovirus Glycoprotein

Zhen-Yong Keck,<sup>b</sup> Sven G. Enterlein,<sup>a</sup> Katie A. Howell,<sup>a</sup> Hong Vu,<sup>a</sup> Sergey Shulenin,<sup>a</sup> Kelly L. Warfield,<sup>a</sup> Jeffrey W. Froude,<sup>c</sup> Nazli Araghi,<sup>a</sup> Robin Douglas,<sup>a</sup> Julia Biggins,<sup>a</sup> Calli M. Lear-Rooney,<sup>c</sup> Ariel S. Wirchnianski,<sup>c</sup> Patrick Lau,<sup>b</sup> Yong Wang,<sup>b</sup> Andrew S. Herbert,<sup>c</sup> John M. Dye,<sup>c</sup> Pamela J. Glass,<sup>c</sup> Frederick W. Holtsberg,<sup>a</sup> Steven K. H. Fong,<sup>b</sup> M. Javad Aman<sup>a</sup>

Integrated BioTherapeutics, Inc., Gaithersburg, Maryland, USA<sup>a</sup>; Department of Pathology, Stanford University, Stanford, California, USA<sup>b</sup>; U.S. Army Medical Research Institute of Infectious Diseases, Frederick, Maryland, USA<sup>c</sup>

## ABSTRACT

Filoviruses cause highly lethal viral hemorrhagic fever in humans and nonhuman primates. Current immunotherapeutic options for filoviruses are mostly specific to Ebola virus (EBOV), although other members of *Filoviridae* such as Sudan virus (SUDV), Bundibugyo virus (BDBV), and Marburg virus (MARV) have also caused sizeable human outbreaks. Here we report a set of pan-ebolavirus and pan-filovirus monoclonal antibodies (MAbs) derived from cynomolgus macaques immunized repeatedly with a mixture of engineered glycoproteins (GPs) and virus-like particles (VLPs) for three different filovirus species. The antibodies recognize novel neutralizing and nonneutralizing epitopes on the filovirus glycoprotein, including conserved conformational epitopes within the core regions of the GP1 subunit and a novel linear epitope within the glycan cap. We further report the first filovirus antibody binding to a highly conserved epitope within the fusion loop of ebolavirus and marburgvirus species. One of the antibodies binding to the core GP1 region of all ebolavirus species and with lower affinity to MARV GP cross neutralized both SUDV and EBOV, the most divergent ebolavirus species. In a mouse model of EBOV infection, this antibody provided 100% protection when administered in two doses and partial, but significant, protection when given once at the peak of viremia 3 days postinfection. Furthermore, we describe novel cocktails of antibodies with enhanced protective efficacy compared to individual MAbs. In summary, the present work describes multiple novel, cross-reactive filovirus epitopes and innovative combination concepts that challenge the current therapeutic models.

## IMPORTANCE

Filoviruses are among the most deadly human pathogens. The 2014–2015 outbreak of Ebola virus disease (EVD) led to more than 27,000 cases and 11,000 fatalities. While there are five species of *Ebolavirus* and several strains of marburgvirus, the current immunotherapeutics primarily target Ebola virus. Since the nature of future outbreaks cannot be predicted, there is an urgent need for therapeutics with broad protective efficacy against multiple filoviruses. Here we describe a set of monoclonal antibodies cross-reactive with multiple filovirus species. These antibodies target novel conserved epitopes within the envelope glycoprotein and exhibit protective efficacy in mice. We further present novel concepts for combination of cross-reactive antibodies against multiple epitopes that show enhanced efficacy compared to monotherapy and provide complete protection in mice. These findings set the stage for further evaluation of these antibodies in nonhuman primates and development of effective pan-filovirus immunotherapeutics for use in future outbreaks.

Filoviruses consisting of Marburg virus (MARV), Ravn virus (RAVV), and five species of ebolavirus, Ebola virus (EBOV), Sudan virus (SUDV), Bundibugyo virus (BDBV), Reston virus (RESTV), and Taï Forest virus (TAFV), are causative agents of severe hemorrhagic fever in humans and nonhuman primates (NHPs) (1, 2). Between 1967 and 2013, 31 filovirus hemorrhagic fever outbreaks have occurred, mainly in central Africa with around 2,000 confirmed cases. Of these 31 outbreaks, 16 were caused by EBOV, and the remaining outbreaks were caused by SUDV, MARV, and BDBV. The unprecedented 2014–2015 Ebola virus disease (EVD) epidemic led to more than 27,000 cases and 11,100 deaths in the first 14 months (<http://apps.who.int/ebola/ebola-situation-reports>). There are currently no approved treatments or vaccines for filoviruses, and most advanced experimental treatments focus only on EBOV. Given that other filoviruses have caused sizeable outbreaks, broadly protective treatment options are urgently needed.

The glycoproteins (GPs) of filoviruses are the main target for antibody-based therapy and vaccination. GP is found in trimeric

form on the virions with each monomer consisting of disulfide-bonded GP1 and GP2 subunits (3). The primary sequences of EBOV and MARV GPs have 30% sequence identity, while the most divergent ebolavirus species (EBOV and SUDV) exhibit 56%

Received 26 August 2015 Accepted 5 October 2015

Accepted manuscript posted online 14 October 2015

**Citation** Keck Z-Y, Enterlein SG, Howell KA, Vu H, Shulenin S, Warfield KL, Froude JW, Araghi N, Douglas R, Biggins J, Lear-Rooney CM, Wirchnianski AS, Lau P, Wang Y, Herbert AS, Dye JM, Glass PJ, Holtsberg FW, Fong SKH, Aman MJ. 2016. Macaque monoclonal antibodies targeting novel conserved epitopes within filovirus glycoprotein. *J Virol* 90:279–291. doi:10.1128/JVI.02172-15.

**Editor:** A. García-Sastre

Address correspondence to M. Javad Aman, javad@integratedbiotherapeutics.com.

Z.-Y.K., S.G.E., and J.A.H. contributed equally to this work.

For a companion article on this topic, see doi:10.1128/JVI.02171-15.

Copyright © 2015, American Society for Microbiology. All Rights Reserved.

GP sequence identity. The sequence identity between filovirus GPs is highest within the receptor binding region (RBR) (4) and GP2, suggesting that shared epitopes may exist within these domains. Several monoclonal antibodies (MAbs) against EBOV GP with protective efficacy in rodents and NHPs have been reported (5–12). Neutralizing antibodies have also been described for SUDV with efficacy in a recently developed rodent model (13, 14). However, these antibodies are species specific and lack cross-neutralizing or cross-protective properties.

Several studies have demonstrated that effective protection of NHPs against EBOV requires polyclonal GP antibodies (5) or cocktails of MAbs (7, 8, 10, 12, 15). A cocktail of three MAbs, ZMapp, protected NHPs when treatment started as late as 5 days postchallenge (12) and is currently in clinical evaluation in Africa. Recently, a set of neutralizing antibodies were isolated from a patient infected with MARV (16), and a neutralization mechanism for these antibodies that is based on blocking the GP interaction with Niemann-Pick C1 (NPC1), the putative filovirus receptor (17, 18), has been proposed (19). One of these MARV antibodies exhibited modest cross-reactivity with EBOV GP ectodomain but failed to neutralize EBOV (16).

Isolation of protective MAbs from humans is ideal, as human antibodies are more likely to be safe. However, human exposure to filoviruses is very limited, and infected patients are likely to mount an immune response that is primarily targeted to the offending strain (20); thus, isolation of high-affinity, cross-reactive filovirus MAbs from infected patients is likely to be difficult. Because NHPs have a close genetic relationship with humans and their immune systems are similar to those of humans, rationally designed experimental immunization using NHPs represents an excellent alternative. Here we describe a vaccination strategy in cynomolgus macaques that resulted in isolation of a set of MAbs with broad reactivity to at least four ebolavirus species, a MAb with pan-filovirus reactivity, and a MAb that neutralized EBOV and SUDV in cell culture. Challenge studies in the mouse model of EVD showed strong protection by several pan-ebolavirus MAbs. Epitope mapping revealed several novel conformational and linear epitopes in the core GP1, the glycan cap, and the fusion domain in GP2. Our findings further describe MAb cocktails that target novel epitope combinations and display enhanced protection against EBOV.

## MATERIALS AND METHODS

**Reagents.** *Saccharomyces cerevisiae* strain EBY-100 (*GAL1-AGA1::URA3 ura3-52 trp1 leu2Δ1 his3Δ200 pep4::HIS2 prb1Δ1.6R can1 GAL*) (Invitrogen, Carlsbad, CA) was maintained in yeast extract-peptone-dextrose (YPD) broth (Difco). The cell culture medium Iscove's modified Dulbecco's medium (IMDM) (Invitrogen, Carlsbad, CA) containing 10% fetal calf serum (FCS) (Sigma-Aldrich Co., St. Louis, MO), 2 mM glutamine, 100 U/ml penicillin, 100 μg/ml streptomycin (Invitrogen, Carlsbad, CA). CpG and interleukin 21 (IL-21) were purchased from Operon (Chicago, IL) and Peprotech (Rocky Hill, NJ). cDNA synthesis reagents were purchased from Invitrogen (Carlsbad, CA). The detecting MAb against the hemagglutinin (HA) tag (phycoerythrin [PE]) used in fluorescence-activated cell sorting (FACS) and MAb against V-5 tag were purchased from Invitrogen (Carlsbad, CA). Micromagnetically activated cell sorting (μMACS) HA-tagged magnetic immunobead and CD20 MicroBeads were purchased from Miltenyi (Auburn, CA). The yeast display vector pYD2 was kindly provided by J. D. Marks (University of California at San Francisco [UCSF]) (21). IgG1-Abvec for full-length immunoglobulin G1 (IgG1) expression was kindly provided by P. Wilson (University of Chicago).

MS40L cells expressing human CD40 ligand (CD40L) was kindly provided by X. M. Luo (Virginia Polytechnic Institute and State University).

**Production and purification of filovirus glycoproteins.** Plasmids containing cDNAs encoding filovirus glycoproteins were generated and expressed in 293T cells. These plasmids contained cDNAs encoding the full ectodomain (GPΔTM) for EBOV and SUDV (amino acids 1 to 627) with an hemagglutinin tag (YPYDVPDYA), followed by a factor 10a cleavage site (IEGRGAR), or truncated forms of EBOV GP (GPΔmuc) (amino acids 1 to 311 linked through an aspartic acid to residues 464 to 637), and SUDV (residues 1 to 313 linked to 474 to 640). GPΔTM proteins were purified as described previously (22), using Q-Sepharose Fast Flow resin. The eluted fractions were pooled, and these fractions were passed over a GE S-200 HR column. S-200 fractions containing GPΔTM were pooled and dialyzed against phosphate-buffered saline (PBS). GPΔmuc protein was purified using Q-Sepharose Fast Flow resin, and eluted fractions containing the proteins were pooled and dialyzed against PBS. For insect cell expression of GPΔTM for EBOV, SUDV, RESTV, and BDBV, baculovirus transfer vectors (pFastBac; Invitrogen) were generated containing the coding regions for residues 1 to 605 followed by a C-terminal 6×His tag under the polyhedrin late promoter and simian virus 40 (SV40) polyadenylation site. Bacmid DNA was produced by *in vivo* transposition in *E. coli* as described previously (23) and used to transfect Sf9 insect cells. The recombinant baculoviruses containing the GPΔTM were recovered from supernatants and amplified in Sf9 cells. The final virus was used to infect Sf9 cells for purification of the proteins from the supernatants 3 days postinfection. After cell debris was removed, the supernatants were concentrated 10 times. The supernatants were mixed with 2 mM CaCl<sub>2</sub>, 0.25 mM Ni<sup>2+</sup>, 20% glycerol, 10 mM imidazole, 0.5% Triton X-100, 1 M NaCl (final concentration), and the pH of the supernatant was adjusted to 7.2 with 5 N NaOH. Ni beads (Ni Sepharose 6 Fast Flow [catalog no. 17-5318-01; GE Lifesciences]) were added to the supernatants at 1 ml per liter of culture volume. Upon overnight incubation at 4°C, beads were separated by centrifugation, resuspended in PBS plus 0.2% Tween 20, and packed into a Bio-Rad Econo-column. The column was washed with the following buffers: PBS (pH 7.1) with 20% glycerol and 0.2% Tween 20, followed by the same buffer containing 10 mM imidazole. Protein was eluted with 500 mM imidazole and dialyzed against PBS with 10% glycerol, arginine, and glutamic acid, pH 7.4. For production of soluble GP (sGP), the full coding sequence of EBOV sGP, including delta peptide followed by a C-terminal 6×His tag was expressed in 293T cells, and supernatant was cleared from delta peptide using a Ni column. The flowthrough was concentrated and used as a source of sGP. Purified proteins were analyzed by bicinchoninic acid (BCA) protein assay, SDS-PAGE, and Western blotting. Proteolytically cleaved GP ectodomains were produced in S2 cells as previously described (19).

**Production of VLPs.** Procedures for production of virus-like particles (VLPs) have been described previously (23). Briefly, cDNAs for GP, nucleoprotein (NP), and VP40 of EBOV, SUDV, or MARV were cloned into pFastBac vector (Life Technologies, Carlsbad, CA), and bacmid DNA was generated and used to transfect Sf9 insect cells. Recombinant baculoviruses were recovered and amplified. VLPs were recovered from the culture supernatants of infected Sf9 cells and purified on sucrose gradients, as published elsewhere (24–27). Before use in animals, VLPs were characterized using assays including total protein (BCA protein assay), identity (Western blotting), electron microscopy, and endotoxin content as described previously (24–27).

**Immunization of cynomolgus macaques.** Two cynomolgus macaques were vaccinated intramuscularly every 4 weeks with 250 μg of trivalent (SUDV, EBOV, and MARV) GPΔmuc formulated in glucopyranosyl lipid adjuvant (GLA) (kindly provided by Immune Design Corp., Seattle, WA), followed by a booster vaccination of 3 mg total of a combination of the trivalent (SUDV, EBOV, and MARV) VLPs along with 50 μg of GLA (Fig. 1). Sera and peripheral blood mononuclear cells (PBMCs) were collected at the same time points. Research was conducted in compliance with the Animal Welfare Act and other federal statutes and regu-

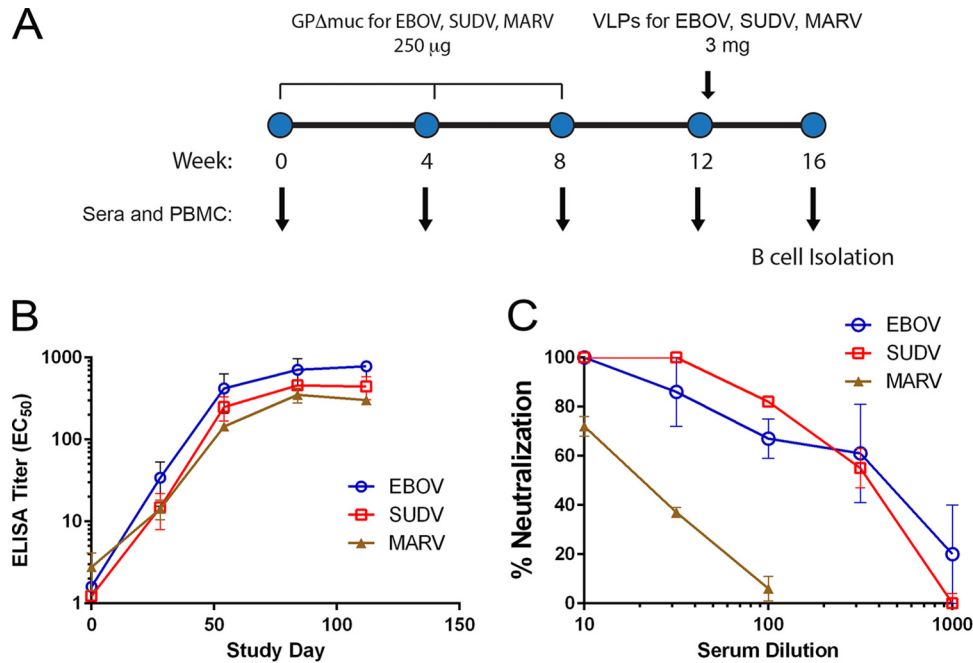


**FIG 1** Immunization study design and antibody response. (A) Immunization and bleed schedule for rhesus macaques. (B) Anti-GP antibody titers (EC<sub>50</sub>) in sera from immunized macaques determined in an ELISA with GPΔTM for the indicated virus species as the antigen. (C) Neutralization titer in macaque sera from day 112 determined using VSV-pseudotyped viruses with EBOV, SUDV, and MARV GP, respectively.

lations relating to animals and experiments involving animals and adhered to principles stated in the *Guide for the Care and Use of Laboratory Animals* (28). The facilities where the research was conducted are fully accredited by the Association for Assessment and Accreditation of Laboratory Animal Care International. Vaccination portions of the studies were conducted under biosafety level 2 (BSL-2) conditions at Smithers-Avanza (Gaithersburg, MD) with all live virus challenges occurring under BSL-4 containment conditions at the U.S. Army Medical Research Institute of Infectious Diseases (USAMRIID). All studies were approved by the Smithers-Avanza Institutional Animal Care and Use Committee (IACUC). All animal housing areas are continuously monitored for temperature and humidity using a state-of-the-art monitoring system, and results are assessed regularly and recorded to ensure animal health and welfare. Animals were individually housed in stainless steel cages and provided environmental enrichment such as mirrors and toys. Animals were supplied with primate diet (Purina 5L07 diet) throughout the study. In addition, animals were also provided with treats such as fresh fruits and vegetables. Water was available *ad libitum* throughout the study. The cynomolgus macaques used in this study were found to be free of antibodies to filovirus, simian T cell leukemia virus type 1 (STLV-1), simian immunodeficiency virus (SIV), and herpesvirus B in testing prior to the start of the study. Blood samples were obtained under anesthesia from the femoral vein of monkeys.

**Isolation and activation of B cells and RNA isolation.** CD20<sup>+</sup> B cells were positively selected with magnetic beads (CD20 Microbeads; Miltenyi Biotec, San Diego, CA) according to the manufacturer's instructions. The B cells were activated, as previously described (29, 30), in IMDM medium containing 10% FCS, 2 mM glutamine, 100 U/ml penicillin, and 100 μl/ml streptomycin and supplemented with 1 μg/ml CpG and 50 ng/ml IL-21 and incubated at 37°C in 5% CO<sub>2</sub> for 13 days. Total RNA from activated B cells was extracted with RNeasy minikit according to the manufacturer's instructions. RNA was used to generate immune yeast antibody libraries.

**Generation of immune yeast antibody library and selection of yeast display ebolavirus GP-scFv.** The methods for generating the yeast display single-chain variable fragment (scFv) library, selection of ebolavirus GP-

specific scFv, and production of IgG1 chimeric macaque-human monoclonal antibodies (M/HMAbs) were as described previously (31). Primers used in primary PCRs to amplify macaque gamma heavy chain and kappa and lambda light chains were described previously (32). Briefly, the yeast library was grown in SG-CAA growth medium (0.51% Na<sub>2</sub>HPO<sub>4</sub>·7H<sub>2</sub>O, 0.43% Na<sub>2</sub>HPO<sub>4</sub>·H<sub>2</sub>O, 0.25% Casamino Acids, 1% galactose) for 48 h at 18 °C. A total of 2 × 10<sup>9</sup> yeast cells were first selected by two rounds of MACS using individual filovirus GPs or a mixture of three filovirus GPs (EBOV, SUDV, and MARV) with or without the mucin domain and followed by two rounds of FACS with 1 × 10<sup>7</sup> MACS output cells. Between each round of selection, the collected cells were grown in SD-CAA medium (same as SG-CAA medium except that it contains dextrose instead of galactose) and induced in SG-CAA medium. Selection was performed using a BD Bioscience FACS Vantage cell sorter. The collected cells were plated on SD-CAA plates.

**Screening for antigen-specific IgG secretion by quantitative ELISA.** B cell supernatants in 96-well plates were collected on day 13 postactivation to test the binding specificity to filovirus glycoproteins by an enzyme-linked immunosorbent assay (ELISA) as described previously (31) with modifications. The wells on the plates were coated with the three GPs (SUDV, EBOV, and MARV) (50 ng/well) at 4°C overnight. The wells were blocked with 2.5% nonfat dry milk and 2.5% normal goat serum. Supernatants (40 μl) collected from 96-well plate were added to the precoated wells. The bound antibodies in the supernatants were detected by human immunoglobulin G (IgG) antibodies conjugated to horseradish peroxidase (HRP) and TMB (3,3',5,5'-tetramethylbenzidine; Sigma) substrate. Absorbance was measured at 450 nm and 570 nm.

**Direct Ig cloning from single B cells.** The genes encoding Ig V<sub>H</sub>, V<sub>κ</sub>, and V<sub>λ</sub> from positive wells were recovered directly using reverse transcription-PCR (RT-PCR) as described previously (33, 34) with the following modifications. cDNA was synthesized in 20 μl per reaction mixture containing first-strand synthesis buffer. Total B cell RNA was reverse transcribed by adding 2 μl of 50 μM random hexamer primers, 1 μl of 10 mM deoxynucleoside triphosphate (dNTP) mix, 0.0625 μl of Igepal CA-630, 40 U of RNase OUT, 2 μl of 0.1 dithiothreitol (DTT), and 50 U of SuperScript III reverse transcriptase. The RT reaction was performed at 42°C for

10 min, 25°C for 10 min, 50°C for 60 min and 94°C for 5 min. The IgH, Igκ, and Igλ V genes were amplified separately by nested PCR starting from 1 μl of cDNA directly following RT and the nested PCR on 1 μl of the first-round PCR product as described previously (32) with the following modifications. All PCRs were performed in a total volume of 20 μl containing nuclease-free water, 4 μl of 5× buffer, 0.4 μl of 10 mM dNTP mix, 0.8 μl of 40 μM mixture of forward and reverse primers (32), and 0.4 μl of PHusion polymerase. The PCR instrument was programmed for 5-min incubation at 94°C, followed by 40 cycles, with one cycle consisting of 30 s at 94°C, 30 s at 55°C (for the first round of PCR) or 60°C (for the nested round of PCR), and 60 s at 70°C, with a final elongation step at 70°C for 7 min before cooling to 4°C. The PCR products were evaluated on 2% agarose gels after the nested PCR. The fragments were purified using a QIAquick gel extraction kit, and cloned into IgG-AbVec, Igκ-AbVec, and Igλ-AbVec containing a murine Ig gene signal peptide sequence and variable-gene cloning sites upstream of the human Igγ1, Igκ, or Igλ constant regions (35).

**Sequence analysis and full IgG conversion.** The primers used to amplify the representative scFv inserts for sequencing were PYDFor (5'-AGT AAC GTT TGT CAG TAA TTG C-3') and PYDRev (5'-GTC GAT TTT GTT ACA TCT ACA C-3'), both located approximately 50 nucleotides outside the scFv inserts on the vector PYDs-A2. The PCR products were sequenced with primer GAP5 (Gap 5; 5'-TTA AGC TTC TGC AGG CTA GTG-3') (Elim Biopharmaceuticals, Inc., Hayward, CA). Sequences were analyzed using the IMGT information system <http://www.imgt.org/> (IMGT/V-Quest) to identify variable region gene segments. Full-length IgG1 were produced and purified as described previously (31).

**Antibody production and purification.** Plasmid carrying genes coding for macaque human chimeric IgH and IgL were mixed with polyethylene amine (catalog no. 23966; Polysciences Inc.) and transfected into HEK 293 cells in suspension in serum-free FreeStyle F17 medium (catalog no. A1383502; Life Technologies). After 7 to 9 days of fermentation, cells were separated by centrifugation, and supernatant was concentrated by tangential flow filtration (TFF). Produced antibodies were captured by protein A (catalog no. 17-0403-01; GE Healthcare), washed, and eluted with 0.1 M glycine buffer (pH 2.4). Fractions containing the Ab peak were collected, neutralized with Ab buffer (20 mM L-histidine [pH 6.0], 150 mM NaCl, and 4% sucrose) and dialyzed against the same buffer overnight at 4°C.

**ELISA.** Nunc MaxiSorp plates (Thermo Fisher Scientific, Waltham, MA) were coated with purified glycoproteins at 100 ng/well and incubated with transfected 293T supernatants or serial dilutions of purified MABs. Bound antibodies were detected using an HRP-conjugated anti-human secondary antibody (KPL, Gaithersburg, MD) and TMB substrate (Life Technologies, Carlsbad, CA). Absorbance values determined at 650 nm were transformed using Softmax 4 parameter curve fit (Molecular Devices, Sunnyvale, CA). The half-maximal effective concentration ( $EC_{50}$ ) value at the inflection point of the curve is reported.

**Competition ELISAs.** Purified C-terminal His-tagged GPΔTM was immobilized at 100 ng/well on 96-well nickel-coated plates (Promega, Madison, WI) at 4°C overnight. The next day, the plates were washed with Dulbecco's phosphate-buffered saline (DPBS) plus 0.05% Tween and blocked for 1 h with blocking buffer T20. FVM02p, FVM04, and FVM20 were biotinylated using EZ-Link NHS-biotin according to the manufacturer's protocol (Life Technologies, Carlsbad, CA). The competing antibodies (all with human Fc) were incubated on coated plates at 20 μg/ml biotinylated MABs or mouse MABs at their respective  $EC_{50}$ . For a control, a set of wells were preincubated with an irrelevant antibody to set the baseline of binding by each detecting MAB. Bound MABs were detected using antistreptavidin antibodies conjugated to HRP (KPL) or anti-mouse antibodies conjugated to HRP and detection with TMB substrate. Absorbance values were determined at 650 nm on a VersaMax plate reader. Percent competition values were calculated from MAB binding in the presence of an irrelevant MAB control and rounded to the nearest whole number.

**Epitope mapping.** Plates were coated with EBOV or SUDV GPΔTM (1 μg/ml) as described above. FVM02p or FVM09 (0.01 μg/ml) was incubated for 1 h with 27 different pools of four or five peptides spanning EBOV or SUDV GPΔTM in blocking buffer at a 100-fold molar excess to the MABs. The peptide-FVM mixture was then added on top of the coated ELISA plates and allowed to bind for 1 h at room temperature. The plates were washed, and bound MABs were detected using goat anti-human antibodies conjugated to HRP (KPL, Gaithersburg, MD) and TMB substrate, and absorbance values were determined at 650 nm on a VersaMax plate reader. A decrease in optical density (OD) compared to the control peptide suggested that the pool contained a peptide with the epitope of the corresponding MAB. These pools were selected for individual peptide screening performed in the same manner as described above.

**VSV pseudotype neutralization assay.** Vero cells were plated at 60,000 cells per well in 96-well plates and incubated overnight at 37°C and 5% CO<sub>2</sub>. The next day, NHP serum was diluted in serum-free Eagle minimum essential medium (EMEM) and mixed independently with vesicular stomatitis virus lacking G protein and expressing various filovirus GP (VSV-GP) (for EBOV, SUDV, and MARV) for 1 h at room temperature. Naive serum was used as a negative control. After 1 h, 100 μl of virus and NHP serum mixture was added to Vero cells, with a final multiplicity of infection (MOI) of 0.04. The plates were incubated for 1 h at 37°C and 5% CO<sub>2</sub> to allow virus to adhere to cells before adding an additional 100 μl of EMEM and incubating at 37°C and 5% CO<sub>2</sub> overnight. Twenty-four hours later, the medium was removed from wells, and cells were lysed with 30 μl of 1× passive lysis buffer (Promega). The plates were rocked at 1.5 rpm for 30 min before the addition of 30 μl of luciferase substrate (Promega). Luminescence was immediately recorded using a TECAN M200 plate reader. Data were fit to a 4PL curve using GraphPad Prism 6. Percent neutralization was calculated based on wells containing virus only.

**High-content imaging-based neutralization assays.** Antibodies were diluted in PBS at 2× the desired final concentrations and mixed with equal volume of live virus (EBOV or SUDV), and the mixture was incubated at 37°C for 1 h before adding to Vero cells in 96-well plates. The cells were incubated with MAB/virus inoculum (MOI of ~1) for 1 h at 37°C and washed with PBS, and growth medium alone without antibody was added to all wells. The cells were fixed at 48 h postinfection, and infected cells were determined by indirect immunofluorescence assay (IFA) using virus-specific MABs and fluorescently labeled secondary antibodies. Percent of infected cells were determined using an Operetta and Harmony software. Data are expressed as the percentage of inhibition relative to control cells treated with vehicle for both EBOV and SUDV.

**Mouse challenge studies.** The lethal mouse-adapted EBOV (MA-EBOV) mouse model was developed at the USAMRIID, using adult mice by serial passages of EBOV in progressively older suckling mice (36–38). Female BALB/c mice (6 to 8 weeks old), were purchased from Charles River Laboratory. Mice were housed in microisolator cages and provided chow and water *ad libitum*. Mice were transferred to a biosafety level 4 containment laboratory at USAMRIID and challenged intraperitoneally (i.p.) with a target of 1,000 PFU of mouse-adapted EBOV. In two independent experiments, groups of mice (with 5 or 10 mice per group) were treated i.p. with different antibodies as indicated in Results. Control mice were challenged but did not receive any treatment. Mice were weighed as groups, and their health was monitored daily for 28 days after infection. Where experimental conditions in independent experiments were the same, the data for those groups were pooled for graphic presentation in figures and statistical analysis.

Animal research was conducted under a protocol approved by the USAMRIID IACUC in compliance with the Animal Welfare Act and other federal statutes and regulations relating to animals and experiments involving animals. The USAMRIID facility is fully accredited by the Association for the Assessment and Accreditation of Laboratory Animal Care International and adheres to the principles stated in the *Guide for the Care and Use of Laboratory Animals* (28). Challenge studies were conducted under maximum containment in an animal biosafety level 4 facility. An-

imal studies were performed in a blind manner (personnel assessing results were unaware of which animals received which treatment). Animals were not specifically allocated or randomized into groups. The number of mice to be used in these studies was selected to measure and determine differences in the levels of protection elicited by the different MAb treatments. Experience with the use of various analyses for determining the probability of differences between control and experimental mouse groups indicates the need for 5 to 10 mice per group. For lethality studies, statistical difference between 0% in the control and  $\geq 30\%$  in the treated groups can be demonstrated using 10 mice per group with  $>90\%$  power using a two-sided alpha level of 0.05. In the cases where large numbers of antibodies were tested in preliminary studies, five mice per group were tested, and then the results were confirmed with the larger group of 10 mice. In these cases, the results of the combination of both studies are shown. To demonstrate statistical differences in the treatment groups, data were analyzed using GraphPad software, version 6 (La Jolla, CA) using the Mantel-Cox log rank test and confirmed using the Gehan-Breslow-Wilcoxon test.

## RESULTS

**Immunization of macaques and generation of broadly reactive antibodies.** Previous efforts toward generation of filovirus MAbs have largely yielded species-specific antibodies against GP. Filovirus GPs are heterodimers of GP1 and GP2 and consist of multiple structural domains. Most of the conserved residues lie within GP2 and RBR (4) of GP1, while a bulky mucin-like domain (MLD) at the C terminus of GP1 is highly variable and known to shield the RBR (22, 39). Because the MLD constitutes the most divergent domain of filovirus GPs, we reasoned that repeated vaccination with a mixture of MLD-deleted GP ectodomains (GP $\Delta$ muc) from three filovirus species would increase the exposure of shared epitopes to the immune system and promote the evolution of broadly reactive antibodies. To this end, two cynomolgus macaques were immunized three times (on days 0, 28, and 56) with a mixture of GP $\Delta$ muc of EBOV, SUDV, and MARV. To further enhance the response, a booster immunization was performed with the highly immunogenic virus-like particles (VLPs) for EBOV, SUDV, and MARV on day 84, and the study was terminated on day 112 (Fig. 1A). Sera were collected prior to each immunization and on the last study day and tested in ELISAs and VSV pseudotype neutralization assays. The NHPs mounted a strong IgG antibody response as measured by ELISAs against EBOV, SUDV, and MARV GP ectodomains lacking the transmembrane region (GP $\Delta$ TM) (Fig. 1B). Neutralization titers were highest against SUDV, followed by EBOV, but significantly lower for MARV (Fig. 1C).

Peripheral blood mononuclear cells (PBMCs) isolated on day 112 from one of the animals (macaque 20667) were used for B cell isolation by CD20-specific magnetic beads and activated as previously described (29, 30). Two approaches were employed to generate MAbs against filovirus GPs: (i) direct Ig gene cloning from single B cells to isolate paired VH and VL antibodies and (ii) high-throughput screening of yeast immune display library. While the first method has the advantage of natural heavy and light chain pairing, the latter method allowed for analysis of a large and more diversified library of heavy and light chain pairing as single-chain variable fragments (scFVs) with different binding affinities to the antigens.

For direct cell cloning, B cells plated at 1 to 4 cells/well and activated in 96-well plates were screened by an ELISA for antigen-specific IgG secretion. A total of 12,000 B cells were analyzed by

ELISAs for binding to GP $\Delta$ TM and GP $\Delta$ muc variants for the three species (SUDV/EBOV/MARV). The vaccinated macaque 20667 serum was used as positive control at a 1:1,000 dilution, and supernatants from wells containing feeder cells only, collected on day 13, were used as negative control. Positive clones were ranked by specific binding as indicated by higher optical density (OD). Out of nine positive clones that bound to the three GPs by ELISAs, two clones showed an OD of  $>1.5$  to GP $\Delta$ muc and approximately 0.5 to 0.7 to GP $\Delta$ TM to at least two species. Heavy and light chain variable Ig genes were amplified by seminested PCR with specific macaque primers (32). After sequencing and reamplifying with cloning primers, the VH and VL PCR fragments were cloned into expression vectors (35) that contain constant region sequences of human Ig $\gamma$ 1 heavy and Ig $\kappa$  light chains. The two full IgG clones were designated FVM01p and FVM02p, and both were primarily ebolavirus-specific antibodies with weak binding to MARV GP (data not shown).

In the second approach, immunoglobulin heavy and light chain variable gene regions were amplified from the RNA isolated from the activated B cells and were constructed into yeast immune display library as described in Materials and Methods. Both triple antigen mixtures (SUDV/EBOV/MARV) GP $\Delta$ muc and GP $\Delta$ TM were used in the selection of antibodies through several rounds of magnetic cell separation and fluorescence-activated cell sorting as previously described (31) and detailed in Materials and Methods. Out of  $>1,000$  monoclonal scFv yeast cells that bound to at least one of the three filovirus GPs, 37 scFvs with reactivity to two filoviruses and unique sequence combinations of heavy and light chain complementarity-determining region 1 (CDR1), CDR2, and CDR3 regions were identified, sequenced, and converted to full IgG1 molecules (macaque variable domain fused to human constant regions). The MAbs were designated FVM03 through FVM29, FVM31 through FVM35, and FVM37 through FVM41. Except for FVM03, which was primarily a MARV-specific antibody, all MAbs bound strongly to both EBOV and SUDV GP and the respective VLPs (data not shown).

**Binding profile of chimeric macaque-human antibodies.** The MAbs were expressed in 293T cells, antibodies in the supernatant were quantified, and their reactivities to GP $\Delta$ TM, GP $\Delta$ muc, and VLPs for EBOV, SUDV, and MARV were determined by ELISAs (data not shown). Upon consideration of the breadth of reactivity, level of expression, and exclusion of nearly identical clones, an initial set of six chimeric antibodies was selected for further characterization: FVM01p, FVM02p, FVM04, FVM09, FVM13, and FVM20. These antibodies were produced, purified, and tested for binding to GP from four ebolavirus species as well as MARV (Mussoko strain). All six MAbs bound tightly to EBOV GP $\Delta$ TM, with EC<sub>50</sub>s ranging from 50 to 100 pM (Fig. 2A). FVM09 and FVM13 showed the strongest binding to all four ebolavirus species, with EC<sub>50</sub>s below 15 ng/ml (100 pM) (Fig. 2A to D). Strong binding to SUDV, BDBV, and RESTV was also observed for FVM02p and FVM04 (Fig. 2B to D). FVM20 and FVM01p showed lower levels of binding to SUDV and RESTV, respectively (Fig. 2B and D). The initial screen of cell supernatants suggested that only FVM02p showed weak binding to MARV GP $\Delta$ TM (data not shown). Recently, we observed that direct coating of the wells on ELISA plates with MARV GP $\Delta$ TM reduced binding of several antibodies specific to MARV GP, while observing higher binding to His-tagged MARV presented on nickel-coated plates (data not shown). Therefore, we tested the binding of several purified MAbs to His-

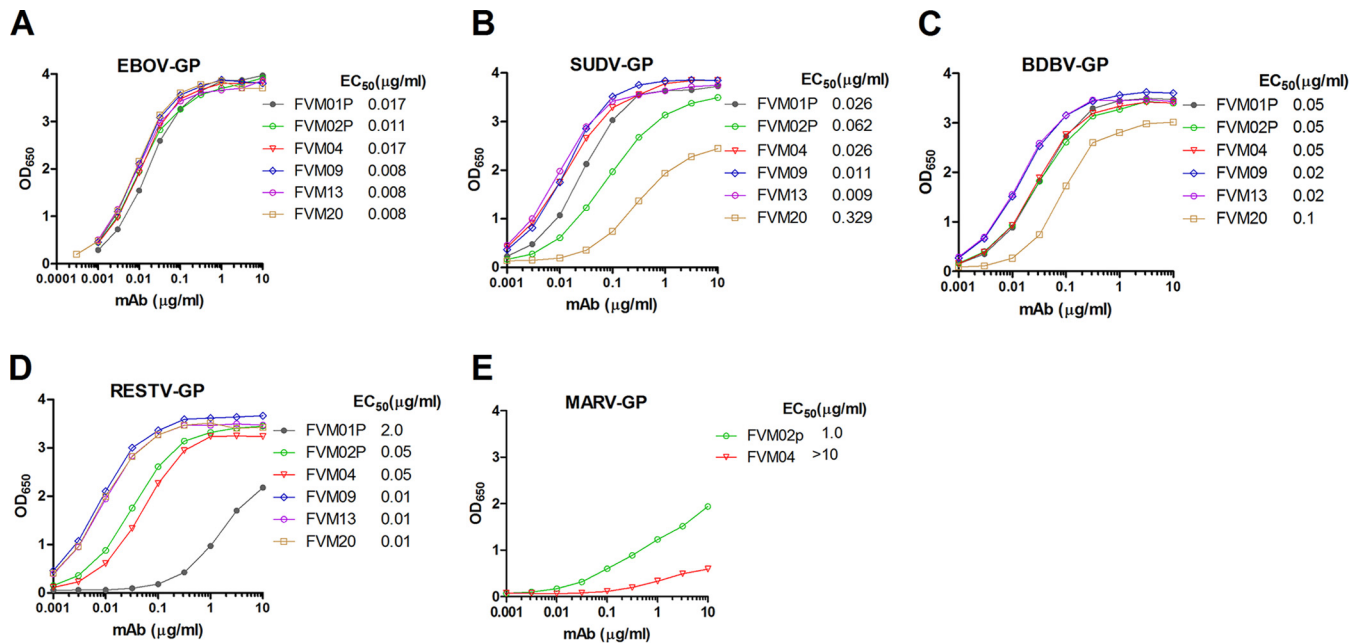


FIG 2 Reactivity of macaque-human chimeric antibodies to filovirus glycoproteins and dose-response binding of the indicated antibodies to GPΔTM of EBOV (A), SUDV (B), BDBV (C), RESTV (D), and MARV (E). Values are optical density at 650 nm (OD<sub>650</sub>) values from three to five ELISA experiments performed over the indicated range of antibody concentrations. The EC<sub>50</sub>s (in micrograms per milliliter) for binding of each antibody to the respective antigen are shown in each panel.

tagged MARV GPΔTM on Ni plates and observed low to moderate binding by FVM02p and FVM04 to MARV (Fig. 2E).

**Epitope mapping.** EBOV GP consists of a receptor-binding GP1 linked by a disulfide bond to GP2, which is responsible for

fusion with the host membrane (Fig. 3A). GP1, in turn, consists of the RBR, glycan cap (GC), and mucin-like domain. The crystal structure of trimeric GP shows that RBR and GC form a chalice-like structure (22) (Fig. 3B, green and blue). GP2 wraps around

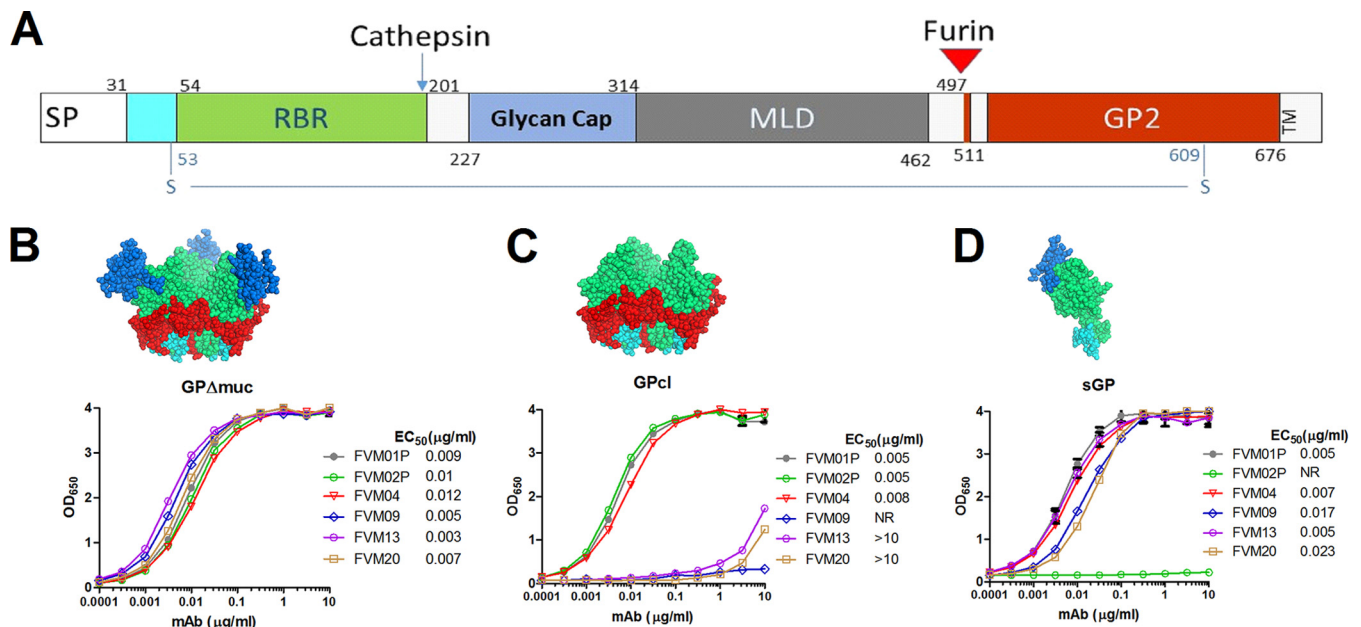


FIG 3 Binding region of pan-ebolavirus antibodies. (A) The domain structure of the EBOV glycoprotein (GenBank accession no. Q05320) is shown. Cathepsin and furin cleavage sites are indicated by arrows. SP, signal peptide; TM, transmembrane. (B) Structure of the MLD-deleted GP (GPΔmuc) (top) and binding of the antibodies to this protein (bottom). (C) Structural representation of EBOV GP after cleavage with thermolysin (top) and reactivity of each antibody to GPcl (bottom). (D) Structure of the EBOV soluble GP (sGP) (top) and its reactivity with the chimeric antibodies (bottom). The N-terminal tail that forms part of the GP base is shown in cyan, and the receptor binding region is shown in green. The glycan cap is shown in blue, and GP2 is shown in red. The EC<sub>50</sub>s (in micrograms per milliliter) for binding of each antibody to the respective antigen are shown in each panel.

TABLE 1 Results of epitope binding competition assay<sup>a</sup>

Detecting MAb <sup>b</sup>	% competition of binding <sup>c</sup> with the following competing antibody:						
	FVM01p	FVM02p	FVM04	FVM09	FVM13	FVM20	c6D8
FVM02p-biotin	None	83	None	None	None	None	None
FVM04-biotin	None	None	82	24	NT	None	None
FVM20-biotin	None	None	23	96	96	77	None
KZ52-biotin	NT	None	None	53	NT	17	None
m13C6	NT	None	76	None	NT	None	None
m2G4	None	None	None	None	None	None	None
m4G7	None	None	None	None	None	None	None
m16G8	None	23	None	None	None	None	None
m8C4	None	18	19	None	None	None	None
m17C6	None	None	91	None	None	None	None
m4B8	None	None	20	None	None	None	None

<sup>a</sup> The antigen (EBOV GPΔTM) coated on ELISA plate was first incubated with the competing antibody at 20 μg/ml before adding the detecting antibody at its respective EC<sub>50</sub>. The percent competition of binding was calculated by comparison to an irrelevant competing antibody. Antibody binding was detected using antistreptavidin antibody conjugated to HRP for the biotinylated antibodies and HRP-conjugated anti-mouse antibodies for untagged primary MABs.

<sup>b</sup> The prefix “m” before the MAB indicates the murine origin of the antibody.

<sup>c</sup> None, less than 15% reduction in binding; NT, not tested.

this structure and along with the N-terminal tail of GP1 forms the base of the chalice (Fig. 3B, red and cyan, respectively). Upon entry in endosomes and cleavage by cathepsins, the GC is removed from this structure; this cleaved GP (GPcl) (Fig. 3C) can be produced *in vitro* using thermolysin (19). During EBOV infection, the unedited GP gene encodes a truncated form of GP with a unique C terminus and a proteolytically cleaved short delta peptide (40, 41). The mature form of this soluble GP (sGP) consists of amino acids 31 to 295, followed by a unique 29-residue C-terminal tail, and lacks both MLD and GP2 but retains most of the GC (Fig. 3D). To determine the overall binding region of the antibodies, we examined the binding of each MAB to GPΔmuc, GPcl, and sGP. As expected, all MABs bound well to GPΔmuc (Fig. 3B), and the binding EC<sub>50</sub>s were comparable to those for GPΔTM (compare with Fig. 1), suggesting that the MLD does not significantly block access to these epitopes. FVM09 failed to bind to GPcl, while binding by FVM13 and FVM20 to GPcl was severely reduced compared to GPΔmuc (Fig. 3C), suggesting that the primary binding site for these three MABs lies within the GC. In contrast, binding of FVM01p, FVM02p, and FVM04 was not affected by removal of the GC (Fig. 3C). Since they all bind to sGP (Fig. 3D), the binding site of these three MABs must lie within residues 31 to 200 in GP1 encompassing the RBR (4). The complete loss of FVM02p binding to sGP (Fig. 3D) indicated that the FVM02p epitope lies within GP2.

To further evaluate potential epitopes, we generated biotinylated FVM02p, FVM04, and FVM20 and tested for competition with unlabeled FVM MABs, ZMapp components c13C6, m2G4, and m4G7 (12), and the neutralizing MAB KZ52 (22) (summarized in Table 1). FVM02-biotin did not compete with any of the antibodies tested, while FVM20 strongly competed with FVM09 and FVM13. KZ52 partially competed with FVM04, FVM09, and FVM20. Partial competition was also observed between FVM04 and m13C6. The competition was also tested for a series of mouse pan-ebolavirus antibodies m16G8, m8C4, m17C6, and m4B8 (the “m” prefix indicates the murine origin of the antibody) that we have recently identified (see the accompanying article by Holtsberg et al. [42]). Except for FVM04 that strongly competed with m17C6, suggesting overlap in the epitope targeted by these two

antibodies, no other competition was observed between the mouse and macaque pan-ebolavirus MABs.

Antibodies were tested for binding to chemically denatured glycoproteins by Western blotting and ELISAs. FVM04 binding to GP was completely lost upon denaturation, while FVM09 and FVM02p binding was not affected. Binding of the other antibodies was reduced but not abrogated (data not shown). On the basis of these data, we concluded that FVM09 and FVM02 react with continuous epitopes, while FVM04 recognizes a conformational epitope, and the epitopes for the other antibodies may contain a linear core with additional discontinuous contact sites.

To identify the linear epitopes for FVM02p and FVM09, we employed a competition assay (as described in Materials and Methods) using overlapping peptides spanning the entire GP sequences for EBOV and SUDV. Peptides sharing the EBOV GP residues 286 to 290 (GEWAF) effectively blocked the binding of FVM09 to EBOV GP (Fig. 4A) and SUDV GP (data not shown). This region is located within a disordered loop connecting β17 and β18 (22) within the glycan cap on the side of the GP chalice (Fig. 4B) and is 100% conserved across all ebolavirus species (Fig. 4C). Using the same approach, we found that peptides containing EBOV GP residues 526 to 535 competed with binding of FVM02p to EBOV GP (Fig. 4D) and SUDV GP (data not shown). This region is located at the tip of the fusion loop in GP2 (22) (Fig. 4E) and is highly conserved within the ebolavirus species (Fig. 4F). Seven out of 10 residues of the putative FVM02p epitope are also identical between ebolavirus and marburgvirus species (Fig. 4F).

**Neutralization of viral entry.** The neutralizing activity of the MABs was first tested in a VSV-GP pseudotype assay in which FVM04 and to a lesser extent FVM09, exhibited neutralizing activity (data not shown). To further confirm these data, we used a high-content imaging-based assay using authentic EBOV and SUDV (described in Materials and Methods). As shown in Fig. 5, significant neutralization of both viruses was observed only for FVM04, while the other MABs failed to neutralize the viruses in this assay.

**Efficacy in mice.** *In vivo* efficacy of the chimeric antibodies was evaluated in BALB/c mice using mouse-adapted EBOV (MA-EBOV) (36). Mice were infected with 1,000 PFU of MA-EBOV

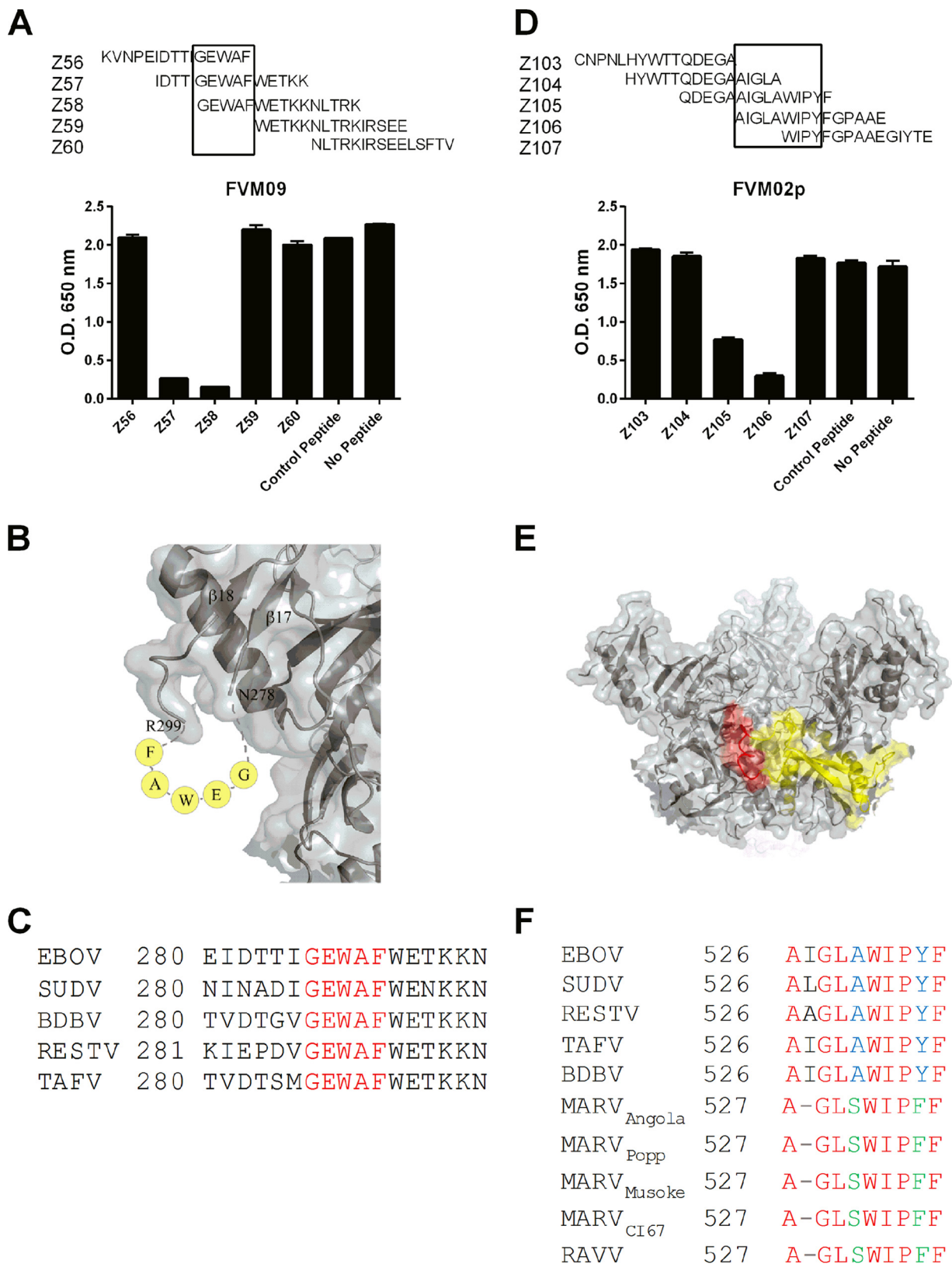


**FIG 4** Epitope mapping of FVM02p and FVM09. Epitopes for FVM02p and FVM09 were determined by competition ELISA using overlapping peptides spanning the full EBOV GP sequence. Peptides were preincubated at 100-fold molar excess with FVM02p or FVM09, and binding of the antibodies in the presence and absence of peptide was determined by ELISAs. (A) Sequences of the five overlapping peptides (top) surrounding the core sequence (boxed) that showed competition with FVM09 binding in an ELISA (bottom). (B) Location of the core FVM09 epitope (yellow circles) within a disordered loop connecting  $\beta$ 17 and  $\beta$ 18 within GP structure (PDB accession no. 3CSY). (C) Sequence identity of the FVM09 epitope and surrounding regions among ebolavirus species. (D) Sequences of the five overlapping peptides (top) surrounding the core sequence (boxed) that showed competition with FVM02p binding in an ELISA (bottom). (E) Position of the core FVM02p epitope within GP fusion loop (PDB accession no. 3CSY). The body of the fusion loop is shown in yellow with its tip containing FVM02p epitope in red. (F) Sequence identity of FVM02p epitope and surrounding regions among ebolavirus species as well as RAVV and MARV strains.

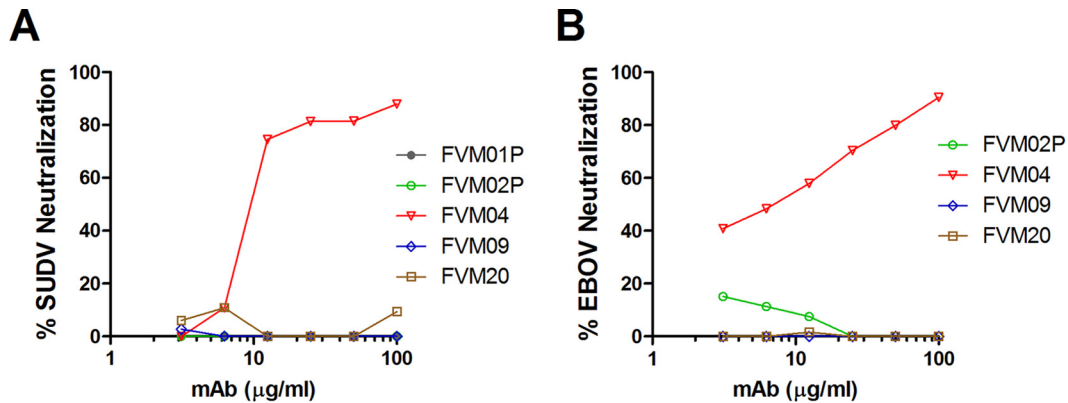


FIG 5 Neutralizing activity of the chimeric antibodies. The neutralizing activity of FVM04, FVM02p, FVM01p, FVM09, and FVM20 were determined for authentic SUDV (A) and EBOV (B) using a high-content imaging assay as described in Materials and Methods.

and treated either with two doses of antibody at 2 h and 3 days postchallenge or with a single dose 3 days postchallenge. All control mice succumbed to infection within 6 to 9 days postinfection, while mice treated twice with FVM04, FVM09, FVM20, or FVM02p showed 100%, 67%, 60%, or 47% survival, respectively (Fig. 6A). In contrast, all the mice treated with FVM01p died from infection (Fig. 6A). Delayed treatment with a single injection of FVM04 3 days after challenge also led to survival of 40% of the mice (Fig. 6A). Animals treated with the protective MABs lost less

weight than control animals and animals treated with FVM01p (Fig. 6B). In particular, mice treated with FVM04 lost no more than 5% weight compared to more than 25% weight loss in controls.

Studies with several EBOV-specific MABs have shown that combinations of several antibodies binding to distinct epitopes enhance the protective efficacy (10, 11, 15), most notably the combination of antibodies binding to the glycan cap and the base of the GP chalice as shown by the remarkable efficacy of ZMapp (12,

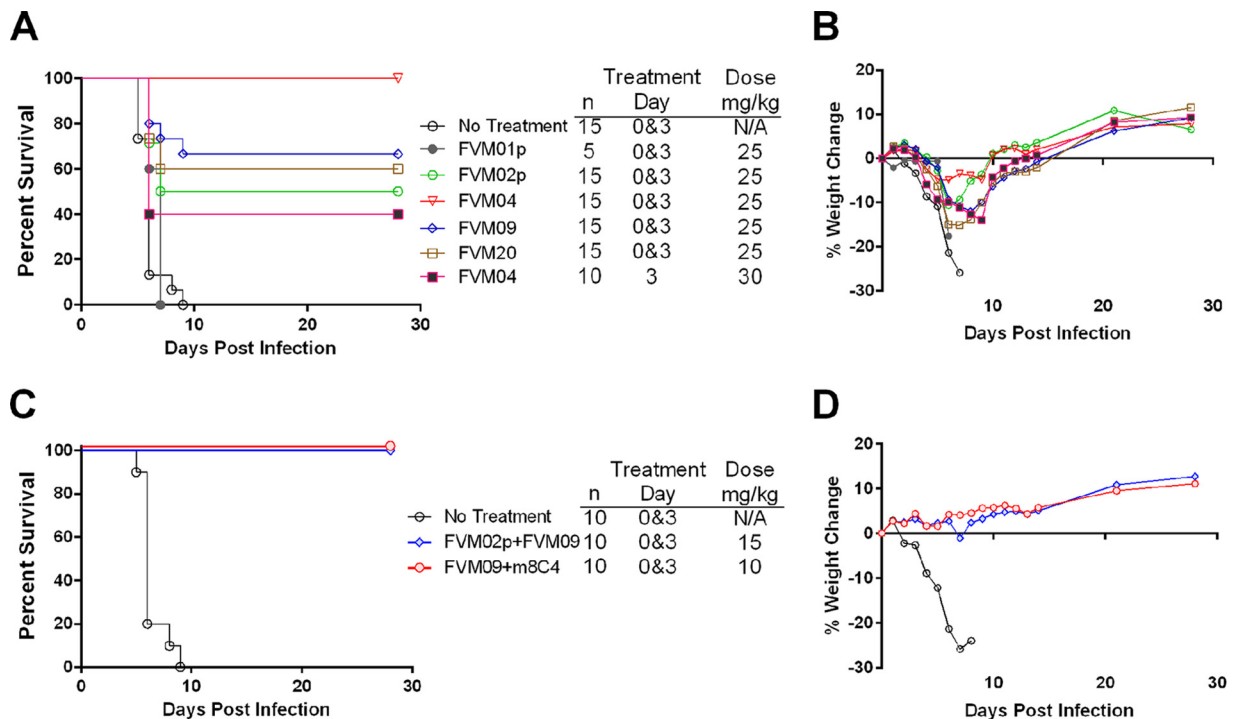
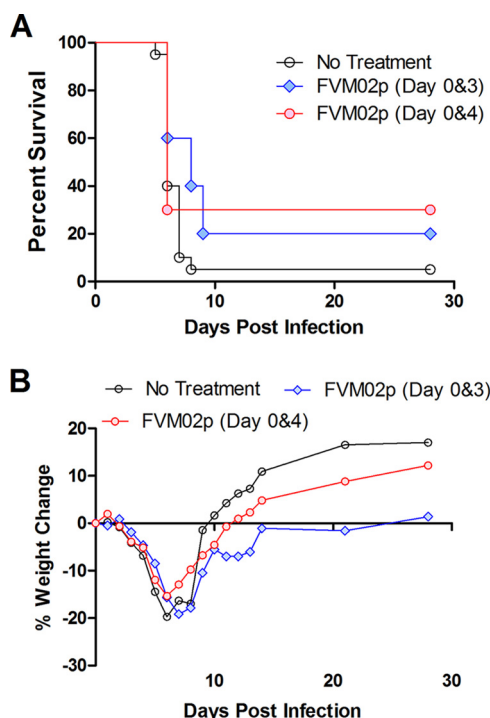


FIG 6 Efficacy of the chimeric antibodies in mouse model of EBOV infection. Mice were infected with 1,000 PFU of MA-EBOV and treated 2 h after infection (day 0) and on day 3 or treated only once on day 3 postinfection as indicated in the panels. (A) Protective efficacy of individual MABs shown as a percentage of survival. Statistical differences were assessed for each treatment group compared to the values for the negative-control group using Mantel-Cox log rank test ( $P$  values of  $<0.3536$  for FVM01p,  $0.0003$  for FVM02p,  $<0.0001$  for FVM04 [days 0 and 3],  $0.0060$  for FVM04 [day 3 only], and  $0.0060$  for FVM09 and FVM20). (B) Percent weight change (group average of surviving animals) after infection and treatment with individual animals from the study shown in panel A. (C) Efficacy of the antibody cocktails shown in the panel. Statistical differences were assessed for each treatment group compared to the negative-control group using the Mantel-Cox log rank test ( $P$  values of  $<0.0001$  for FVM02p plus FVM09 and  $<0.0001$  for FVM09 plus m8C4). (D) Percent weight change in animals treated with antibody cocktails shown in panel C. The number of animals ( $n$ ), antibody dose, and treatment regimen in each group are shown for each study.



**FIG 7** Efficacy of FVM02p in mouse model of MARV. Mice were infected with 1,000 PFU of MA-MARV and treated either 2 h after infection (day 0) and on day 3 or at 2 h and 3 days as indicated in the panels. (A) Percent survival of challenged mice. (B) Percent weight change (group average of surviving animals) after infection and treatment with individual animals from the study shown in panel A.

43). Thus, we sought to determine whether combination of our pan-ebolavirus antibodies that bind to novel epitopes will lead to enhanced efficacy compared to individual MABs. To this end, we tested two different combinations: (i) FVM02p and FVM09, targeting the fusion loop and glycan cap, respectively; and (ii) FVM09 and m8C4, a mouse pan-ebolavirus antibody (see the accompanying article by Holtsberg et al. [42]), which binds to a conformational epitope involving the glycan cap. Both of these combinations provided 100% protection against lethal challenge although the antibodies were administered at a lower dose compared to the study with individual antibodies (Fig. 6C). Notably, mice treated with the MAb cocktails showed no sign of disease or weight loss but gained weight after infection (Fig. 6D).

Although FVM02p binding to MARV GPΔTM was very low (Fig. 2E), we tested the efficacy of FVM02p in a mouse model of Marburg virus infection. In two experiments, we observed 20% and 30% protection from lethal challenge when mice were treated with FVM02p on days 0 and 3 or days 0 and 4, respectively (Fig. 7); however, the protection was not statistically significant.

## DISCUSSION

The current EVD epidemic in West Africa affected far more people than all previously recorded outbreaks combined. Beside EBOV, other filoviruses, such as SUDV, BDBV, and MARV, have caused sizeable outbreaks in the past 48 years. The unprecedented 2014–2015 EBOV outbreak highlights the need for broadly effective treatment options and a cross-protective vaccine, as the nature of the next filovirus outbreak cannot be predicted. Antibodies

represent promising treatment options for filovirus hemorrhagic fever (39). However, most published therapeutic MABs are strictly specific for EBOV (6, 8–10, 12, 15, 44, 45), and only a few, closely related, SUDV-specific MABs have been reported (13, 14, 46).

We used a novel prime-boost immunization strategy in macaques to focus the immune response to conserved epitopes of the filovirus GP, including the RBR and GP2, expecting a higher percentage of pan-filovirus antibodies. Sera from immunized macaques showed broad reactivity that neutralized SUDV-GP and EBOV-GP, but not MARV-GP, VSV-pseudotyped viruses efficiently. We identified a set of broadly reactive pan-ebolavirus MABs with strong binding to EBOV, SUDV, BDBV, and RESTV GP; two MABs also exhibited weak binding to MARV GP. Thus, it appears that by using this regimen, the B cell response has been dominated by ebolavirus-specific epitopes.

The most protective MAB, FVM04, exhibited balanced binding at subnanomolar concentrations to four ebolavirus species tested and effectively neutralized EBOV and SUDV. Interestingly, FVM04 also shows weak binding to MARV, suggesting that further engineering of this MAB may lead to an effective pan-filovirus antibody. In a mouse model of EBOV infection, FVM04 was fully protective when used in two doses. Importantly, a single treatment given 3 days postinfection (peak of viremia in mice [36]) resulted in significant protection ( $P = 0.006$ ). FVM04 binds to a conformational epitope within the core of GP1 (residues 31 to 200), a region that encompasses the RBR and the base of GP1 (22). While previous reports of antibodies targeting the GP1 core indicated that epitopes in this region are likely concealed (16, 19; also see the accompanying article by Holtsberg et al. [42]), the FVM04 binding profile was not significantly changed upon removal of the MLD, suggesting that the epitope of FVM04 is well exposed and likely on the top of the trimeric GP chalice. Interestingly, FVM01p, another MAB that strongly bound the GP1 core, failed to protect mice, indicating that the specificity of the epitope is critical for protection.

In this study, we report the first filovirus antibody targeting the fusion loop (FL) within GP2. This MAB (FVM02p) binds with subnanomolar  $EC_{50}$ s to EBOV, SUDV, BDBV, and RESTV GP. The core linear epitope consists of residues 526 to 535 within GP2 at the tip of the FL that is nearly 100% conserved among all ebolavirus species. Crystallography data show that this region makes several contacts with residues within the RBR in the prefusion structure of EBOV GP (22). Interestingly, the FVM02p epitope is also 75% conserved between ebolavirus species and marburgvirus, and consistent with this, FVM02p also bound with reduced affinity to MARV GP. FVM02p provided significant protection from lethal MA-EBOV challenge in mice ( $P = 0.0003$ ) and a low level of protection, albeit statistically insignificant, in MARV-infected mice. It is possible that further engineering of the FVM02p complementarity-determining regions (CDRs) may lead to higher binding affinity to MARV GP, potentially leading to an effective pan-filovirus MAB. Given the lack of neutralization, the mechanism of action of FVM02p remains to be determined. It is possible that *in vitro* neutralization assays in Vero cells may be poorly indicative of *in vivo* neutralization, which can be also dependent on Fc-mediated effector functions.

In addition, we are reporting another set of MABs that primarily target a novel linear epitope within the glycan cap. FVM09, FVM13, and FVM20 effectively bound to a core hydrophobic peptide within the glycan cap that is 100% conserved among all ebo-

lavirus GP molecules. In contrast to FVM09 binding to GP that was completely blocked by an excess of GEWAF-containing peptides, this competition was partial against FVM13 and FVM20 (data not shown). Consistently, low levels of FVM13 and FVM20 binding to GPcl (GP lacking the glycan cap) were detected, suggesting that these two MABs have additional contact sites within GP1, while FVM09 binding is completely dependent on the glycan cap. While FVM09 did not neutralize EBOV and SUDV, low level of neutralization was observed in VSV pseudotype assay (data not shown). When tested in mice, FVM09 and FVM20 provided partial, but significant ( $P < 0.0001$ ), protection against EBOV. Thus, these MABs represent novel protective epitopes primarily focused on the glycan cap. It is noteworthy that the only neutralizing MAB identified in this study (FVM04) is a conformational antibody, suggesting the complex nature of epitopes that need to be targeted for effective neutralization of virus entry.

Our findings are consistent with previous studies of EBOV MABs indicating that a cocktail of MABs targeting key epitopes provides greater protective efficacy (6–8, 10, 12, 15, 43, 47). We tested two different cocktails of two MABs which, when used alone, were only partially protective. A cocktail of FVM09 and FVM02p provided 100% protection at 15 mg/kg of body weight ( $P < 0.0001$ ), while each individual MAB at 25 mg/kg was only partially protective. Similarly, full protection ( $P < 0.0001$ ) was observed when the glycan cap binder FVM09 was combined with a partially protective mouse MAB (m8C4 [see the accompanying article by Holtsberg et al. {42}]) at 10 mg/kg. Remarkably, mice treated with these cocktails showed no symptoms or weight loss. Previously described efficacious, EBOV-specific cocktails targeted epitopes on the glycan cap and MLD (MB-003 [7, 8]) or on the glycan cap and base (ZMab [15, 48]) and ZMapp [12]. Our results demonstrate that novel combinations of epitopes, distinct from those targeted by ZMapp and MB-003, with a conserved profile can be targeted for effective protection against filoviruses. The mechanism of the enhancement resulting from antibody combinations remains to be defined and may include synergistic effects of neutralization and effector functions.

In summary, our findings indicate the presence of well-exposed conformational and linear conserved epitopes that can be targeted for treatment of hemorrhagic fever caused by multiple ebolavirus species. Furthermore, we report antibody combinations targeting novel epitopes that can be utilized for development of effective pan-ebolavirus and potentially pan-filovirus MAB cocktails. Future evaluation of these cocktails in NHPs should pave the way toward clinical development of broadly protective filovirus treatments.

## ACKNOWLEDGMENTS

This work was supported by a contract (HDTRA1-13-C-0015) from the U.S. Defense Threat Reduction Agency (DTRA) to M.J.A. and by a grant (R43AI098178) from the National Institute of Allergy and Infectious Diseases (NIAID) to S.G.E.

We thank Erica Sapphire and Marnie Fusco of the Scripps Research Institute for providing cleaved GP, Gary Kobinger of the Public Health Agency of Canada for providing m2G4 and m4G7, and Larry Zeitlin of Mapp Biopharmaceutical for providing c13C6.

Research was conducted under an IACUC-approved protocol in compliance with the Animal Welfare Act, PHS policy, and other federal statutes and regulations relating to animals and experiments involving animals. The facility where this research was conducted is accredited by the Association for Assessment and Accreditation of Laboratory Animal Care

International and adheres to the principles stated in the 2011 *Guide for the Care and Use of Laboratory Animals*. Opinions, interpretations, conclusions, and recommendations are those of the authors and are not necessarily endorsed by the U.S. Army.

## FUNDING INFORMATION

HHS | NIH | National Institute of Allergy and Infectious Diseases (NIAID) provided funding to Sven G Enterlein under grant number R43AI098178. DOD | Defense Threat Reduction Agency (DTRA) provided funding to M. Javad Aman under grant number HDTRA1-13-C-0015.

## REFERENCES

1. Feldmann H, Kiley MP. 1999. Classification, structure, and replication of filoviruses. *Curr Top Microbiol Immunol* 235:1–21.
2. Kuhn JH, Andersen KG, Baize S, Bao Y, Bavari S, Berthet N, Blinkova O, Brister JR, Clawson AN, Fair J, Gabriel M, Garry RF, Gire SK, Goba A, Gonzalez JP, Gunther S, Happi CT, Jahrling PB, Kapetshi J, Kobinger G, Kugelman JR, Leroy EM, Maganga GD, Mbala PK, Moses LM, Muyembe-Tamfum JJ, N'Faly M, Nichol ST, Omilabu SA, Palacios G, Park DJ, Paweska JT, Radoshitzky SR, Rossi CA, Sabeti PC, Schieffelin JS, Schoepp RJ, Sealfon R, Swanepoel R, Towner JS, Wada J, Wauquier N, Yozwiak NL, Formenty P. 2014. Nomenclature- and database-compatible names for the two Ebola virus variants that emerged in Guinea and the Democratic Republic of the Congo in 2014. *Viruses* 6:4760–4799. <http://dx.doi.org/10.3390/v6114760>.
3. Volchkov VE, Feldmann H, Volchkova VA, Klenk HD. 1998. Processing of the Ebola virus glycoprotein by the proprotein convertase furin. *Proc Natl Acad Sci U S A* 95:5762–5767. <http://dx.doi.org/10.1073/pnas.95.10.5762>.
4. Kuhn JH, Radoshitzky SR, Guth AC, Warfield KL, Li W, Vincent MJ, Towner JS, Nichol ST, Bavari S, Choe H, Aman MJ, Farzan M. 2006. Conserved receptor-binding domains of Lake Victoria marburgvirus and Zaire ebolavirus bind a common receptor. *J Biol Chem* 281:15951–15958. <http://dx.doi.org/10.1074/jbc.M601796200>.
5. Dye JM, Herbert AS, Kuehne AI, Barth JF, Muhammad MA, Zak SE, Ortiz RA, Prugar LI, Pratt WD. 2012. Postexposure antibody prophylaxis protects nonhuman primates from filovirus disease. *Proc Natl Acad Sci U S A* 109:5034–5039. <http://dx.doi.org/10.1073/pnas.1200409109>.
6. Marzi A, Yoshida R, Miyamoto H, Ishijima M, Suzuki Y, Higuchi M, Matsuyama Y, Igarashi M, Nakayama E, Kuroda M, Saijo M, Feldmann F, Brining D, Feldmann H, Takada A. 2012. Protective efficacy of neutralizing monoclonal antibodies in a nonhuman primate model of Ebola hemorrhagic fever. *PLoS One* 7:e36192. <http://dx.doi.org/10.1371/journal.pone.0036192>.
7. Olinger GG, Jr, Pettitt J, Kim D, Working C, Bohorov O, Bratcher B, Hiatt E, Hume SD, Johnson AK, Morton J, Pauly M, Whaley KJ, Lear CM, Biggins JE, Scully C, Hensley L, Zeitlin L. 2012. Delayed treatment of Ebola virus infection with plant-derived monoclonal antibodies provides protection in rhesus macaques. *Proc Natl Acad Sci U S A* 109:18030–18035. <http://dx.doi.org/10.1073/pnas.1213709109>.
8. Pettitt J, Zeitlin L, Kim DH, Working C, Johnson JC, Bohorov O, Bratcher B, Hiatt E, Hume SD, Johnson AK, Morton J, Pauly MH, Whaley KJ, Ingram MF, Zovanyi A, Heinrich M, Piper A, Zelko J, Olinger GG. 2013. Therapeutic intervention of Ebola virus infection in rhesus macaques with the MB-003 monoclonal antibody cocktail. *Sci Transl Med* 5:199ra113. <http://dx.doi.org/10.1126/scitranslmed.3006608>.
9. Qiu X, Alimonti JB, Melito PL, Fernando L, Stroher U, Jones SM. 2011. Characterization of Zaire ebolavirus glycoprotein-specific monoclonal antibodies. *Clin Immunol* 141:218–227. <http://dx.doi.org/10.1016/j.clim.2011.08.008>.
10. Qiu X, Audet J, Wong G, Pillet L, Bello A, Cabral T, Strong JE, Plummer F, Corbett CR, Alimonti JB, Kobinger GP. 2012. Successful treatment of ebola virus-infected cynomolgus macaques with monoclonal antibodies. *Sci Transl Med* 4:138ra81. <http://dx.doi.org/10.1126/scitranslmed.3003876>.
11. Qiu X, Fernando L, Melito PL, Audet J, Feldmann H, Kobinger G, Alimonti JB, Jones SM. 2012. Ebola GP-specific monoclonal antibodies protect mice and guinea pigs from lethal Ebola virus infection. *PLoS Negl Trop Dis* 6:e1575. <http://dx.doi.org/10.1371/journal.pntd.0001575>.
12. Qiu X, Wong G, Audet J, Bello A, Fernando L, Alimonti JB, Fausther-Bovendo H, Wei H, Aviles J, Hiatt E, Johnson A, Morton J,

- Swope K, Bohorov O, Bohorova N, Goodman C, Kim D, Pauly MH, Velasco J, Pettitt J, Olinger GG, Whaley K, Xu B, Strong JE, Zeitlin L, Kobinger GP. 2014. Reversion of advanced Ebola virus disease in nonhuman primates with ZMapp. *Nature* 514:47–53. <http://dx.doi.org/10.1038/nature13777>.
13. Chen G, Koellhoffer JF, Zak SE, Frei JC, Liu N, Long H, Ye W, Nagar K, Pan G, Chandran K, Dye JM, Sidhu SS, Lai JR. 2014. Synthetic antibodies with a human framework that protect mice from lethal Sudan ebolavirus challenge. *ACS Chem Biol* 9:2263–2273. <http://dx.doi.org/10.1021/cb5006454>.
  14. Dias JM, Kuehne AI, Abelson DM, Bale S, Wong AC, Halfmann P, Muhammad MA, Fusco ML, Zak SE, Kang E, Kawaoka Y, Chandran K, Dye JM, Saphire EO. 2011. A shared structural solution for neutralizing ebolaviruses. *Nat Struct Mol Biol* 18:1424–1427. <http://dx.doi.org/10.1038/nsmb.2150>.
  15. Qiu X, Audet J, Wong G, Fernando L, Bello A, Pillet S, Alimonti JB, Kobinger GP. 2013. Sustained protection against Ebola virus infection following treatment of infected nonhuman primates with ZMab. *Sci Rep* 3:3365. <http://dx.doi.org/10.1038/srep03365>.
  16. Flyak AI, Ilinykh PA, Murin CD, Garron T, Shen X, Fusco ML, Hashiguchi T, Bornholdt ZA, Slaughter JC, Sapparapu G, Klages C, Ksiazek TG, Ward AB, Saphire EO, Bukreyev A, Crowe JE, Jr. 2015. Mechanism of human antibody-mediated neutralization of marburg virus. *Cell* 160:893–903. <http://dx.doi.org/10.1016/j.cell.2015.01.031>.
  17. Carette JE, Raaben M, Wong AC, Herbert AS, Obernosterer G, Mulherkar N, Kuehne AI, Kranzusch PJ, Griffin AM, Ruthel G, Dal Cin P, Dye JM, Whelan SP, Chandran K, Brummelkamp TR. 2011. Ebola virus entry requires the cholesterol transporter Niemann-Pick C1. *Nature* 477:340–343. <http://dx.doi.org/10.1038/nature10348>.
  18. Cote M, Misasi J, Ren T, Bruchez A, Lee K, Filone CM, Hensley L, Li Q, Ory D, Chandran K, Cunningham J. 2011. Small molecule inhibitors reveal Niemann-Pick C1 is essential for Ebola virus infection. *Nature* 477:344–348. <http://dx.doi.org/10.1038/nature10380>.
  19. Hashiguchi T, Fusco ML, Bornholdt ZA, Lee JE, Flyak AI, Matsuoka R, Kohda D, Yanagi Y, Hammel M, Crowe JE, Jr, Saphire EO. 2015. Structural basis for marburg virus neutralization by a cross-reactive human antibody. *Cell* 160:904–912. <http://dx.doi.org/10.1016/j.cell.2015.01.041>.
  20. Maruyama T, Rodriguez LL, Jahrling PB, Sanchez A, Khan AS, Nichol ST, Peters CJ, Parren PW, Burton DR. 1999. Ebola virus can be effectively neutralized by antibody produced in natural human infection. *J Virol* 73:6024–6030.
  21. Razai A, Garcia-Rodriguez C, Lou J, Geren IN, Forsyth CM, Robles Y, Tsai R, Smith TJ, Smith LA, Siegel RW, Feldhaus M, Marks JD. 2005. Molecular evolution of antibody affinity for sensitive detection of botulinum neurotoxin type A. *J Mol Biol* 351:158–169. <http://dx.doi.org/10.1016/j.jmb.2005.06.003>.
  22. Lee JE, Fusco ML, Hessel AJ, Oswald WB, Burton DR, Saphire EO. 2008. Structure of the Ebola virus glycoprotein bound to an antibody from a human survivor. *Nature* 454:177–182. <http://dx.doi.org/10.1038/nature07082>.
  23. Warfield KL, Dye JM, Wells JB, Unfer RC, Holtsberg FW, Shulenin S, Vu H, Swenson DL, Bavari S, Aman MJ. 2015. Homologous and heterologous protection of nonhuman primates by Ebola and Sudan virus-like particles. *PLoS One* 10:e0118881. <http://dx.doi.org/10.1371/journal.pone.0118881>.
  24. Bavari S, Bosio CM, Wiegand E, Ruthel G, Will AB, Geisbert TW, Hevey M, Schmaljohn C, Schmaljohn A, Aman MJ. 2002. Lipid raft microdomains: a gateway for compartmentalized trafficking of Ebola and Marburg viruses. *J Exp Med* 195:593–602. <http://dx.doi.org/10.1084/jem.20011500>.
  25. Warfield KL, Bosio CM, Welcher BC, Deal EM, Mohamadzadeh M, Schmaljohn A, Aman MJ, Bavari S. 2003. Ebola virus-like particles protect from lethal Ebola virus infection. *Proc Natl Acad Sci U S A* 100:15889–15894. <http://dx.doi.org/10.1073/pnas.2237038100>.
  26. Swenson DL, Warfield KL, Kuehl K, Larsen T, Hevey MC, Schmaljohn A, Bavari S, Aman MJ. 2004. Generation of Marburg virus-like particles by co-expression of glycoprotein and matrix protein. *FEMS Immunol Med Microbiol* 40:27–31. [http://dx.doi.org/10.1016/S0928-8244\(03\)00273-6](http://dx.doi.org/10.1016/S0928-8244(03)00273-6).
  27. Warfield KL, Swenson DL, Negley DL, Schmaljohn AL, Aman MJ, Bavari S. 2004. Marburg virus-like particles protect guinea pigs from lethal Marburg virus infection. *Vaccine* 22:3495–3502. <http://dx.doi.org/10.1016/j.vaccine.2004.01.063>.
  28. National Research Council. 2011. Guide for the care and use of laboratory animals, 8th ed. National Academies Press, Washington, DC.
  29. Brocca-Cofano E, McKinnon K, Demberg T, Venzon D, Hidajat R, Xiao P, Daltabuit-Test M, Patterson LJ, Robert-Guroff M. 2011. Vaccine-elicited SIV and HIV envelope-specific IgA and IgG memory B cells in rhesus macaque peripheral blood correlate with functional antibody responses and reduced viremia. *Vaccine* 29:3310–3319. <http://dx.doi.org/10.1016/j.vaccine.2011.02.066>.
  30. Huang J, Doria-Rose NA, Longo NS, Laub L, Lin CL, Turk E, Kang BH, Migueles SA, Bailer RT, Mascola JR, Connors M. 2013. Isolation of human monoclonal antibodies from peripheral blood B cells. *Nat Protoc* 8:1907–1915. <http://dx.doi.org/10.1038/nprot.2013.117>.
  31. Keck ZY, Xia J, Wang Y, Wang W, Krey T, Prentoe J, Carlsen T, Li AY, Patel AH, Lemon SM, Bukh J, Rey FA, Founk SK. 2012. Human monoclonal antibodies to a novel cluster of conformational epitopes on HCV E2 with resistance to neutralization escape in a genotype 2a isolate. *PLoS Pathog* 8:e1002653. <http://dx.doi.org/10.1371/journal.ppat.1002653>.
  32. Sundling C, Phad G, Douagi I, Navis M, Karlsson Hedestam GB. 2012. Isolation of antibody V(D)J sequences from single cell sorted rhesus macaque B cells. *J Immunol Methods* 386:85–93. <http://dx.doi.org/10.1016/j.jim.2012.09.003>.
  33. Liao HX, Levesque MC, Nagel A, Dixon A, Zhang R, Walter E, Parks R, Whitesides J, Marshall DJ, Hwang KK, Yang Y, Chen X, Gao F, Munshaw S, Kepler TB, Denny T, Moody MA, Haynes BF. 2009. High-throughput isolation of immunoglobulin genes from single human B cells and expression as monoclonal antibodies. *J Virol Methods* 158:171–179. <http://dx.doi.org/10.1016/j.jviromet.2009.02.014>.
  34. Tiller T, Meffre E, Yurasov S, Tsuiji M, Nussenzweig MC, Wardemann H. 2008. Efficient generation of monoclonal antibodies from single human B cells by single cell RT-PCR and expression vector cloning. *J Immunol Methods* 329:112–124. <http://dx.doi.org/10.1016/j.jim.2007.09.017>.
  35. Smith K, Garman L, Wrammert J, Zheng NY, Capra JD, Ahmed R, Wilson PC. 2009. Rapid generation of fully human monoclonal antibodies specific to a vaccinating antigen. *Nat Protoc* 4:372–384. <http://dx.doi.org/10.1038/nprot.2009.3>.
  36. Bray M, Davis K, Geisbert T, Schmaljohn C, Huggins J. 1998. A mouse model for evaluation of prophylaxis and therapy of Ebola hemorrhagic fever. *J Infect Dis* 178:651–661. <http://dx.doi.org/10.1086/515386>.
  37. Bray M, Davis K, Geisbert T, Schmaljohn C, Huggins J. 1999. A mouse model for evaluation of prophylaxis and therapy of Ebola hemorrhagic fever. *J Infect Dis* 179(Suppl 1):S248–S258. <http://dx.doi.org/10.1086/514292>.
  38. Gibb TR, Bray M, Geisbert TW, Steele KE, Kell WM, Davis KJ, Jaax NK. 2001. Pathogenesis of experimental Ebola Zaire virus infection in BALB/c mice. *J Comp Pathol* 125:233–242. <http://dx.doi.org/10.1053/jcpa.2001.0502>.
  39. Saphire EO. 2013. An update on the use of antibodies against the filoviruses. *Immunotherapy* 5:1221–1233. <http://dx.doi.org/10.2217/imt.13.124>.
  40. Sanchez A, Trappier SG, Mahy BW, Peters CJ, Nichol ST. 1996. The virion glycoproteins of Ebola viruses are encoded in two reading frames and are expressed through transcriptional editing. *Proc Natl Acad Sci U S A* 93:3602–3607. <http://dx.doi.org/10.1073/pnas.93.8.3602>.
  41. Volchkov VE, Becker S, Volchkova VA, Ternovoj VA, Kotov AN, Netesov SV, Klenk HD. 1995. GP mRNA of Ebola virus is edited by the Ebola virus polymerase and by T7 and vaccinia virus polymerases. *Virology* 214:421–430. <http://dx.doi.org/10.1006/viro.1995.0052>.
  42. Holtsberg FW, Shulenin S, Vu H, Howell KA, Patel SJ, Gunn B, Karim M, Lai JR, Frei JC, Nyakatura EK, Zeitlin L, Douglas R, Fusco ML, Froude JW, Saphire EO, Herbert AS, Wirchnianski AS, Lear-Rooney CM, Alter G, Dye JM, Glass PJ, Warfield KL, Aman MJ. 2016. Pan-ebolavirus and pan-filovirus mouse monoclonal antibodies: protection against ebolavirus and Sudan virus. *J Virol* 90:000–000. <http://dx.doi.org/10.1128/JVI.02171-15>.
  43. Murin CD, Fusco ML, Bornholdt ZA, Qiu X, Olinger GG, Zeitlin L, Kobinger GP, Ward AB, Saphire EO. 2014. Structures of protective antibodies reveal sites of vulnerability on Ebola virus. *Proc Natl Acad Sci U S A* 111:17182–17187. <http://dx.doi.org/10.1073/pnas.1414164111>.
  44. Olinger GG, Bailey MA, Dye JM, Bakken R, Kuehne A, Kondig J, Wilson J, Hogan RJ, Hart MK. 2005. Protective cytotoxic T-cell responses induced by Venezuelan equine encephalitis virus replicons ex-

- pressing Ebola virus proteins. *J Virol* 79:14189–14196. <http://dx.doi.org/10.1128/JVI.79.22.14189-14196.2005>.
45. Wilson JA, Hevey M, Bakken R, Guest S, Bray M, Schmaljohn AL, Hart MK. 2000. Epitopes involved in antibody-mediated protection from Ebola virus. *Science* 287:1664–1666. <http://dx.doi.org/10.1126/science.287.5458.1664>.
  46. Brannan JM, Froude JW, Prugar LI, Bakken RR, Zak SE, Daye SP, Wilhelmsen CE, Dye JM. 2015. Interferon alpha/beta receptor-deficient mice as a model for Ebola virus disease. *J Infect Dis* 212(Suppl 2):S282–S294. <http://dx.doi.org/10.1093/infdis/jiv215>.
  47. Qiu X, Wong G, Fernando L, Ennis J, Turner JD, Alimonti JB, Yao X, Kobinger GP. 2013. Monoclonal antibodies combined with adenovirus-vectored interferon significantly extend the treatment window in Ebola virus-infected guinea pigs. *J Virol* 87:7754–7757. <http://dx.doi.org/10.1128/JVI.00173-13>.
  48. Qiu X, Wong G, Fernando L, Audet J, Bello A, Strong J, Alimonti JB, Kobinger GP. 2013. mAbs and Ad-vectored IFN-alpha therapy rescue Ebola-infected nonhuman primates when administered after the detection of viremia and symptoms. *Sci Transl Med* 5:207ra143. <http://dx.doi.org/10.1126/scitranslmed.3006605>.